Molecular Biology of the Cell
Vol. 20, 1478–1492, March 1, 2009

Mutant Huntingtin Impairs Post-Golgi Trafficking to Lysosomes by Delocalizing Optineurin/Rab8 Complex from the Golgi Apparatus

Daniel del Toro,*† Jordi Alberch,*† Francisco Lázaro-Diéguez,*‡ Raquel Martín-Ibáñez,*† Xavier Xifró,*† Gustavo Egea,*‡ and Josep M. Canals*†

*Departament de Biologia Cel·lular, Immunologia i Neurociències, Facultat de Medicina, IDIBAPS, Universitat de Barcelona, E-08036 Barcelona, Spain; †Centro de Investigación Biomédica en Red sobre Enfermedades Neurodegenerativas (CIBERNED), Spain; and ‡Institut de Nanotecnologia, Universitat de Barcelona, E-08036 Barcelona, Spain

Submitted July 16, 2008; Revised December 22, 2008; Accepted January 6, 2009
Monitoring Editor: Robert G. Parton

Huntingtin regulates post-Golgi trafficking of secreted proteins. Here, we studied the mechanism by which mutant huntingtin impairs this process. Colocalization studies and Western blot analysis of isolated Golgi membranes showed a reduction of huntingtin in the Golgi apparatus of cells expressing mutant huntingtin. These findings correlated with a decrease in the levels of optineurin and Rab8 in the Golgi apparatus that can be reverted by overexpression of full-length wild-type huntingtin. In addition, immunoprecipitation studies showed reduced interaction between mutant huntingtin and optineurin/Rab8. Cells expressing mutant huntingtin produced both an accumulation of clathrin adaptor complex 1 at the Golgi and an increase of clathrin-coated vesicles in the vicinity of Golgi cisternae as revealed by electron microscopy. Furthermore, inverse fluorescence recovery after photobleaching analysis for lysosomal-associated membrane protein-1 and mannose-6-phosphate receptor showed that the optineurin/Rab8-dependent post-Golgi trafficking to lysosomes was impaired in cells expressing mutant huntingtin or reducing huntingtin levels by small interfering RNA. Accordingly, these cells showed a lower content of cathepsin D in lysosomes, which led to an overall reduction of lysosomal activity. Together, our results indicate that mutant huntingtin perturbs post-Golgi trafficking to lysosomal compartments by delocalizing the optineurin/Rab8 complex, which, in turn, affects the lysosomal function.

INTRODUCTION

Huntington's disease (HD) is a neurodegenerative disorder caused by abnormal polyglutamine expansion in the N-terminal part of the huntingtin (htt) protein (Kremer *et al*., 1994), which produces significant dysfunction and neural death, especially in the medium spiny neurons of the striatum. Htt is a huge protein with a widespread distribution in neurons, including cell bodies, dendrites and axons (Sharp *et al*., 1995). Detailed subcellular fractionation and microscopic studies have shown that htt is also associated with vesicles and microtubules (Difiglia *et al*., 1995; Hoffner *et al*., 2002), where it interacts with molecular motors that promote the transport of vesicles containing brain derived-neurotrophic factor (BDNF) (Gauthier *et al*., 2004). We previously demonstrated that htt also participates in post-Golgi trafficking of proteins that follow the regulated secretory pathway (del Toro *et al*., 2006). Thus, mutant htt (mhtt) impairs post-Golgi trafficking, which in turn decreases the number of vesicles containing BDNF, thereby contributing to a reduced trophic support that is essential for striatal neurons during HD progression (Canals *et al*., 2004). However, the molecular mechanism by which htt participates in post-Golgi trafficking remains unclear. Htt colocalizes with the Golgi apparatus and with exocytic vesicles (Difiglia *et al*., 1995) and reduced expression of htt by RNA interference (RNAi) disrupts the Golgi apparatus (Caviston *et al*., 2007). Moreover, several htt-interacting proteins, such as HIP14 (Singaraja *et al*., 2002) and optineurin (Hattula and Peranen, 2000), contribute to the function of the Golgi apparatus and exocytosis.

Optineurin, a Rab8 effector (Hattula and Peranen, 2000), colocalizes with htt in the Golgi apparatus where it contributes to post-Golgi trafficking and Golgi organization (Sahlender *et al*., 2005). Rab8 belongs to the family of Rab GTPases, central regulators of vesicle budding, motility, and fusion (for review, see Stenmark and Olkkonen, 2001; Pfeffer, 2003). Optineurin and Rab8 form a complex that participates in the regulation of the post-Golgi transport of proteins, the sorting of which is mediated by the clathrin adaptor complex 1 (AP-1) (Sahlender *et al*., 2005; Au *et al*., 2007).

Here, we examined whether htt regulates post-Golgi transport via the optineurin/Rab8 complex in striatal-derived cells that express wild-type (wt) full-length htt (with 7Q, wt cells) or full-length mhtt (with 111Q, mhtt cells). We demonstrate that mhtt cells show reduced levels of htt in the Golgi apparatus, which in turn presents decreased levels of

This article was published online ahead of print in *MBC in Press* (http://www.molbiolcell.org/cgi/doi/10.1091/mbc.E08–07–0726) on January 14, 2009.

Address correspondence to: Dr. Josep M. Canals (jmcanals@ub.edu).

Abbreviations used: AP-1, clathrin adaptor complex 1; CCV, clathrin-coated vesicle; GT, galactosyltransferase; htt, huntingtin; Lamp, lysosome-associated membrane protein; LcB, clathrin light chain B; MPR, mannose-6-phosphate receptor; TGN, *trans*-Golgi network; VSV-G, *vesicular stomatitis virus glycoprotein*.

optineurin and Rab8. This combination leads to reduced clathrin-dependent post-Golgi trafficking to lysosomes. Therefore, mhtt affects post-Golgi transport to the plasma membrane (del Toro *et al*., 2006) and to lysosomes by uncoupling the optineurin/Rab8 complex at late Golgi compartments.

MATERIALS AND METHODS

Reagents and Antibodies

Anti-htt monoclonal antibody 2166 was from Millipore Bioscience Research Reagents (Temecula, CA). Anti-GM130, anti-Rab8, and anti-γ-adaptin antibodies were from BD Biosciences Transduction Laboratories (Lexington, KY), and anti-optineurin and anti-lysosomal–associated membrane protein (Lamp)-1 antibodies were from Abcam (Cambridge, MA). The anti-cathepsin D antibody was a generous gift from Dr. William Brown (Cornell University, Ithaca, NY). Fluorescent Cy3 (anti-rabbit), Cy2 (anti-mouse), and Alexa 647 (anti-mouse and -rabbit) secondary antibodies were from Invitrogen (Carlsbad, CA) and Texas Red-conjugated anti-mouse antibody was from Jackson ImmunoResearch Laboratories (West Grove, PA). Lipofectamine 2000 was from Invitrogen. All other reagents used were from Sigma-Aldrich (St. Louis, MO).

DNA Constructs

Lamp-1 fused to red fluorescent protein (RFP) was kindly supplied by Dr. Walther Mothes (Yale University School of Medicine, New Haven, CT). The mannose-6-phosphate receptor (MPR) fused to green fluorescent protein (GFP) and clathrin light chain B (LcB) fused to yellow fluorescence protein (YFP) were generously supplied by Dr. Juan S Bonifacino (National Institutes of Health, Bethesda, MD). Galactosyltransferase (GT) fused to YFP or cyan fluorescence protein (CFP) was kindly supplied by Dr. Jennifer Lippincott-Schwartz (National Institutes of Health). The Rab8 and Rab8 Q67L construct fused to GFP was supplied by Dr. Ira Mellman (Yale University School of Medicine). *Vesicular stomatitis virus glycoprotein* (VSV-G) fused to GFP was kindly provided by Kai Simons (Max Planck Institute of Molecular Cell Biology and Genetics, Dresden, Germany). Full-length 17Q htt (FL-17Q-htt) and full-length 75Q htt (FL-75Q-htt) were gifts from Drs. Fréderic Saudou and Sandrine Humbert (Institut Curie, Orsay, France).

Striatal-derived wt and mhtt, M213, Primary Striatal Cultures, and Transfection

To study the role of htt in post-Golgi trafficking, we used the following cell lines: striatal knockin cells stably expressing full-length htt (7Q/7Q, wt cells) or full-length mhtt (111Q/111Q, mhtt cells) established from HdhQ111 knockin mice (Trettel *et al*., 2000). M213 cells, a conditionally immortalized rat striatal derived neural stem cells (Giordano *et al*., 1993). Both cells were grown in Dulbecco's modified Eagle's medium supplemented with 10% fetal bovine serum, 100 U/ml penicillin, 100 μg/ml streptomycin, 2 mM L-glutamine, and 1 mM sodium pyruvate. For primary striatal cultures, certified time pregnant B6CBA mice (Charles River Laboratories, Les Oncins, France) were deeply anesthetized on gestational day 14.5 (E14.5) and fetuses (E0.5, day of vaginal plug) were rapidly removed from the uterus by cesarean section. Fetal brains were then excised and placed in sterile phosphate-buffered saline (PBS), pH 7.4. The striatal primordia were dissected bilaterally, pooled and gently dissociated with a fire-polished Pasteur pipet. Cells were plated onto 24-well plates containing glass coverslips precoated with 0.1 mg/ml poly-D-lysine (Sigma-Aldrich) at a density of 150,000 cells/cm^2. We obtained a neuronal culture growing the cells in Eagle's minimum essential medium (Invitrogen) supplemented with B27 (Invitrogen). The plates were placed in an incubator at 37°C in a 5% CO_2 atmosphere. Cells were transfected using Lipofectamine 2000, following the manufacturer's instructions.

Full-length htt constructs with 17 or 75 polyQ tracts (FL-17Q-htt and FL-75Q-htt, respectively) were cotransfected (8:1) with GT-YFP, which selectively marks the Golgi apparatus. As a control condition, cells were transfected with GT-YFP alone. Cells transfected with FL-17Q-htt or FL-75Q-htt were selected on the basis of their increased immunoreactivity for anti-htt antibody because there is no tag in these vectors. Rab8 Q67L-GFP was also cotransfected with GT-CFP (8:1), and as a control condition GT-CFP was transfected alone.

Small Interfering RNA (siRNA) Transfection

For silencing htt, RNA duplexes targeted four different regions of mouse htt gene (GenBank accession no. NM_010414): 5′-agagcuaggcacacugcucat-3′, 5′-aaaacuacccucuggaugugg-3′, 5′-uuaacaaggcuugucccaaag-3′, 5′-acaacatctgtacaattgcag-3′ as described previously (Caviston *et al*., 2007). Control cells were transfected with nontargeting RNA duplex oligonucleotides. Twenty-four hours after plating cells on coverslips, cells were cotransfected with 60 nM htt siRNA or control siRNA and GT-YFP or MPR-GFP by using Lipofectamine 2000, following the manufacturer's instructions. All experiments were performed 72 h after transfection.

Electron Microscopy

Striatal knockin cells were rapidly washed in prewarmed (37°C) 0.1 M PIPES buffer, pH 7.4, and then fixed with 1.25% glutaraldehyde in PIPES buffer containing 2% sucrose and 2 mM Mg_2SO_4 for 1 h at room temperature. They were then gently scraped, pelleted at 100*g* for 10 min, rinsed three times in PIPES buffer, and postfixed with 1% (wt/vol) OsO_4, 1% (wt/vol) $K_3Fe(CN)_6$ in PIPES buffer for 1 h in the dark. Cells were then treated for 5 min with 0.1% tannic acid, dehydrated with graded ethanol solutions, and finally embedded in Epon plastic resin. Ultrathin sections (50–70 nm thick) were stained with lead citrate and observed on a JEOL 1010 electron microscope. Micrographs of 20–25 randomly selected fields were obtained with a Bioscan digital camera (Gatan, Munich, Germany). The density of clathrin-coated vesicle (CCV) profiles was measured by dividing the total number of CCV profiles by the cytoplasmic area (square micrometers) of each field. Results are expressed as the mean ± SD.

Immunofluorescence Staining and Confocal Microscopy Analysis

At 24 h posttransfection, cells were fixed in 4% paraformaldehyde for 10 min, 0.2 M glycine for 20 min, and then permeabilized in 0.1% saponin for 10 min. Blocking was done in 1% bovine serum albumin (BSA) in PBS for 1 h. Specimens were incubated with primary antibodies: anti-GM130 (1:250), anti-htt (1:100), anti-optineurin (1:100), anti-rab8 (1:100), anti-γ-adaptin (1:100), anti-Lamp-1 (1:100), and anti-cathepsin D (1:100). Thereafter, samples were incubated with the following secondary antibodies: Cy2-conjugated anti-mouse (1:200), Cy3-conjugated anti-rabbit (1:300), Texas Red-conjugated anti-mouse (1:300), or anti-mouse or anti-rabbit Alexa 647 (1:200). In some cultures, nuclei were counterstained with the fluorescent dye ToPro-3 (Invitrogen).

Double-stained cells were examined by confocal microscopy using a TCS SL laser scanning confocal spectral microscope (Leica Microsystems Heidelberg, Mannheim, Germany) with argon and HeNe lasers attached to a DMIRE2 inverted microscope (Leica Microsystems Heidelberg). Images were taken using a 63× numerical aperture objective with a 4× digital zoom and standard (1 Airy disk) pinhole. For each cell, the entire three-dimensional stack of images from the ventral surface to the top of the cell was obtained by using the Z drive in the TCS SL microscope. The size of the optical image was 0.5 μm. Colocalization was measured by using the "colocalization" plug-in of the freeware ImageJ version 1.33 by Wayne Rasband (National Institutes of Health). Briefly, for each cell stack, the cell area was delineated and the total number of double-positive pixels for htt, optineurin, Rab8, or γ-adaptin, and a specific subcellular region for each slice was summed. This value was divided by the number of total positive pixels for htt, optineurin, Rab8, or γ-adaptin in the stack, and multiplied by 100.

For the quantitation of MPR-GFP–containing structures, we measured those fluorescent spots composed of between 2 and 20 pixels (both included, 108-1080 nm). In all cases, 20–30 cells were randomly selected from at least three independent cultures.

Staining of Lysosomes and Autophagic Vacuoles

Lysosomes were labeled by incubating the cells with 1 μM LysoTracker Red DND-99 (Invitrogen) for 30 min at room temperature. Thereafter, cells were washed in PBS and fixed as described above. Given that in our images 1 pixel represents 54 nm, we considered a lysosome to be any fluorescent spot positive for LysoTracker and mad up of between 6 and 40 pixels (from 324 to 2160 nm inclusive). For staining of autophagic vacuoles, a monodansylcadaverine (MDC) stock solution (20 mM) was diluted 1:400 in PBS and applied to the cells for 15 min. Cells were washed with PBS and incubated 30 min with medium containing 1 μM LysoTracker. Thereafter, cells were washed in PBS and fixed as described above.

Inverse Fluorescence Recovery after Photobleaching Analysis Experiments

iFRAP experiments were carried out using the Leica confocal microscope described previously equipped with an incubation system with temperature and CO_2 control. Cells (3.5×10^5) were seeded on a 35-mm plates (NUNC A/S, Roskilde, Denmark), each with a glass coverslip of 22 mm (Microcoverglass; Electron Microscopy Sciences, Hatfield, PA). After 24 h, cells were transfected with 4 μg of Lamp-1-RFP, MPR-GFP, LcB-YFP, or VSV-G-GFP constructs. For full-length htt constructs, FL-17Q-htt or FL-75Q-htt constructs were cotransfected (100:1) with MPR-GFP. At 24 h posttransfection, cells were incubated with 0.1 mg/ml cycloheximide in culture medium for 2 h at 20°C. Subsequently, the glass coverslips holding transfected cells was mounted in the videoconfocal chamber, and temperature was warmed to 33°C.

For visualization of RFP, CFP, GFP, and YFP, images were acquired using a 63× oil immersion objective lens (numerical aperture, 1.32), by using either a 514-nm laser line (for RFP), a 488-nm laser line (for GFP/YFP), or a 458-nm laser line (for CFP); excitation beam splitter RSP 500; emission range detection

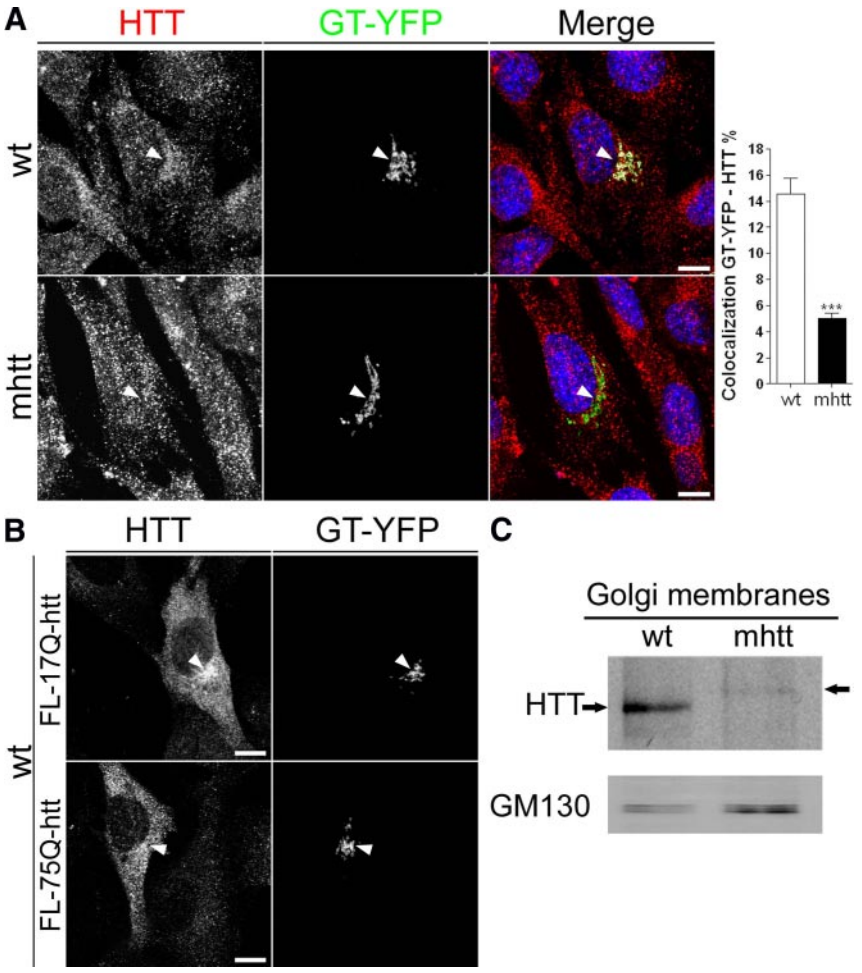

Figure 1. mhtt cells showed reduced protein levels and localization of mhtt in the Golgi apparatus. (A) Colocalization of htt with GT-YFP, which marks the Golgi complex, revealed lower colocalization of htt with GT-YFP in mhtt cells compared with wt cells. (B) wt cells transfected with FL-17Q-htt showed increased localization of htt with GT-YFP respect to those transfected with FL-75Q-htt. (C) Representative Western blot of isolated Golgi membranes showing reduced htt protein levels in mhtt cells. Fifteen micrograms of Golgi membranes was loaded in each line. Results are represented as a mean ± SEM determined from the analysis of three independent experiments (***$p < 0.001$). Images represent the projection of the two slices containing the maximal cross-section of the cell nucleus. Bar, 8 μm.

500–600 nm; and a confocal pinhole set at 2–3 Airy units to minimize changes in fluorescence efficiency caused by fluorescence proteins moving away from the plane of focus.

The whole cytoplasmic area of the transfected cell was photobleached using 80 scans with the 514- or 488-nm laser line at full power. Images were then collected in stream mode every 5 s during 10 min for RFP or 20 min for GFP/YFP.

All iFRAP data were corrected and normalized using the equation described in Dundr *et al*. (2002) (also see Supplemental Material). iFRAP curves were modeled equally well with a two-phase exponential decay equation (Supplemental Figure 1). Nine to 12 cells were randomly selected from at least three independent transfections. All cells expressed similar levels of tagged proteins to render the data comparable.

Isolation of Golgi Membranes

Golgi fractions from knockin cells were prepared at 4°C as described in Balch *et al*. (1984), with few modifications (Fernandez-Ulibarri *et al*., 2007). Briefly, twenty-two 100-mm plates (NUNC A/S) per condition were pelleted and washed twice in cold PBS (10 min at 500 × *g*) and lysis buffer (10 mM Tris-HCl, 0.25 M sucrose, 1 mM phenylmethylsulfonyl fluoride [PMSF], 10 μg/ml aprotinin, and 1 μg/ml leupeptin, pH 7.4). The cell pellet was then resuspended in 4 volumes of lysis buffer and homogenized using the Ball-Balch homogenizer device. The homogenate was brought to a sucrose concentration of 37% (wt/vol) by adding 62% (wt/vol) sucrose in 10 mM Tris-HCl, pH 7.4, and EDTA (1 mM, final concentration). Fifteen millimeter of this solution was placed at the bottom of a SW 28 ultracentrifuge tube and carefully overlaid with 10 ml of sucrose at 35% (wt/vol) and 10 ml sucrose at 29% (wt/vol) in 10 mM Tris-HCl, pH 7.4. Gradients were centrifuged at 25,000 rpm for 2.5 h. The Golgi-enriched membrane fraction was recovered at the 35–29% sucrose interphase and subsequently stored at −80°C. Protein concentration was determined by detergent-compatible protein assay (Bio-Rad, Hercules, CA).

Western Blot Analysis

Total protein extracts were prepared from striatal cell cultures by homogenization in lysis buffer (50 mM Tris base, 150 mM NaCl, 2 mM EDTA, 50 mM NaF, 1% NP-40, 1 mM PMSF, 10 μg/ml aprotinin, and 1 μg/ml leupeptin, pH 7.4). Samples were centrifuged at 10,000 × *g* for 10 min, and the protein contents were determined as described above. Proteins from total extracts (20 μg for optineurin or Rab8 and 30 μg for cathepsin D analyses) or proteins from Golgi membranes (15 μg for htt and 10 μg for optineurin or Rab8 analyses) were resuspended in 5× SDS sample buffer (62.5 mM phosphate buffer, 50% glycerol, 12.5% SDS, 16.7 mM dithiothreitol, and 1.2 mM Bromophenol blue, pH 7.0), boiled for 5 min, resolved by 6 or 12% SDS-polyacrylamide gel electrophoresis (PAGE), and transferred to Immobilon-P transfer membranes (Millipore, Billerica, MA). Blots were blocked in 5% nonfat powdered milk and 5% BSA in Tris-buffered saline/Tween 20 (TBS-T: 50 mM Tris-HCl, 150 mM NaCl, pH 7.4, and 0.05% Tween 20) for 1 h at room temperature. The membranes were then incubated overnight at 4°C with anti-htt (1:1000), anti-optineurin (1:500), anti-Rab8 (1:1000), or anti-cathepsin D (1:1000) antibodies. Membranes were then rinsed three times in TBS-T and incubated with horseradish peroxidase-conjugated secondary antibody for 1 h at room temperature. After washing the membranes for 30 min with TBS-T, they were developed using the enhanced chemiluminescence substrate kit (GE Healthcare, Uppsala, Sweden). The phoretix densitometry program (Phoretix International, Newcastle, United Kingdom) was used to quantify the htt, optineurin, Rab8, and cathepsin D bands. Values are given as the mean ± SEM.

Immunoprecipitation

Immunoprecipitation was performed by incubation of total protein extracts (as described above; 300 μg) with 1 μg of anti-Rab8 antibody overnight at 4°C followed by a 4-h incubation with 50 μl of protein A-Sepharose Cl-4B (Sigma-Aldrich). The beads were washed by centrifugation three times and then boiled for 10 min in 10 μl of 5× SDS sample buffer. The immunocomplexes were resolved on 6 or 12% SDS-PAGE and transferred to Immobilon-P transfer membranes. Western blot analysis was carried out as described above.

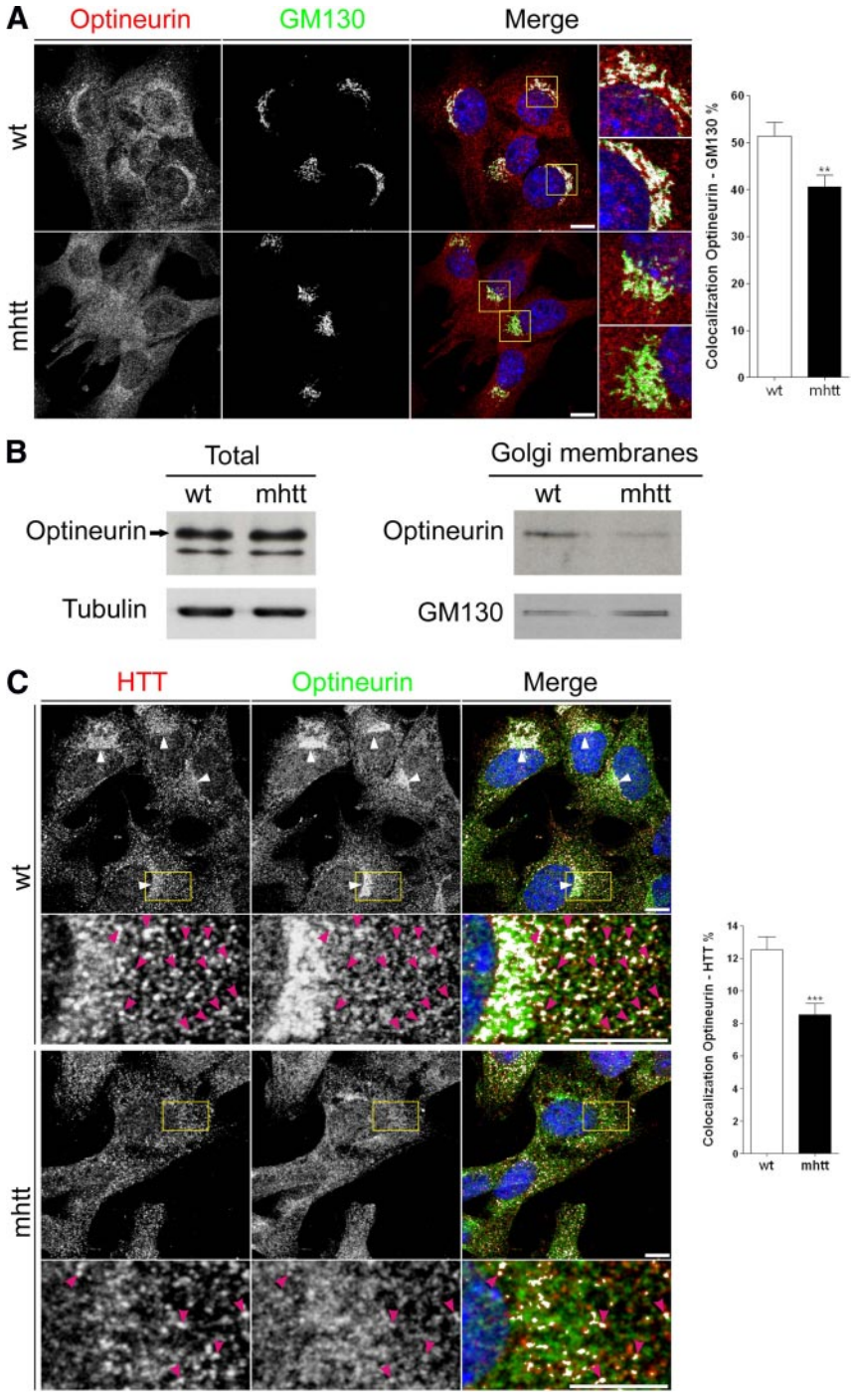

Figure 2. mhtt cells showed delocalization of optineurin in the Golgi apparatus. (A) Colocalization between optineurin and GM130, a Golgi marker, revealed reduced localization of optineurin in the Golgi apparatus of mhtt compared with wt cells. (B) Representative Western blot showing similar optineurin protein levels in total extracts of wt and mhtt cells (20 μg each line) but reduced optineurin protein levels in isolated Golgi membranes in mhtt cells (10 μg each line). (C) Colocalization studies showed reduced colocalization between htt and optineurin in mhtt cells compared with wt cells. wt cells showed colocalization of htt and optineurin at the Golgi complex (arrowheads). Pink arrowheads indicate vesicles containing both proteins (enlarged region). mhtt cells showed reduced localization of htt and optineurin at the Golgi apparatus and lower colocalization of both proteins (enlarged region, pink arrowheads). Results are represented as a mean ± SEM determined from the analysis of three independent experiments (**$p < 0.01$; ***$p < 0.001$). Images represent the projection of the two slices containing the maximal cross section of the cell nucleus. Bar, 8 μm.

Blots were incubated with anti-htt (1:1000), anti-optineurin (1:1000), and anti-Rab8 (1:1000) and detected using enhanced chemiluminescent reagents.

Proteolysis Assays

Cells (5×10^4/well) were seeded on a 24-well plate (NUNC A/S) containing a glass coverslip of 12 mm. After 24 h, cells were washed with PBS, and 500 μl per well of medium containing 25 μg/ml the quenched fluorescent substrate DQ-collagen IV (Invitrogen) was added. After 2 h, cells were fixed, and the fluorescent degradation products of DQ-collagen IV were observed in the Leica TCS SL laser scanning confocal spectral microscope, as described above.

Statistical Analysis

GraphPad Prism version 4.0 (GraphPad software, San Diego, CA) software was used to perform unpaired *t* test or one-way analysis of variance and Bonferroni post hoc test. For iFRAP experiments, the nonparametric *t* test followed by the Mann–Whitney test was used.

RESULTS

mhtt Is Delocalized from the Golgi Apparatus

Htt is a cytosolic protein that has been associated not only with the Golgi apparatus (Difiglia *et al.*, 1995; Caviston *et al.*, 2007) but also with exocytic vesicles (Gauthier *et al.*, 2004). To study the mechanism by which mhtt impairs post-Golgi trafficking, we first performed colocalization studies between htt and GT-YFP, which specifically labels the Golgi

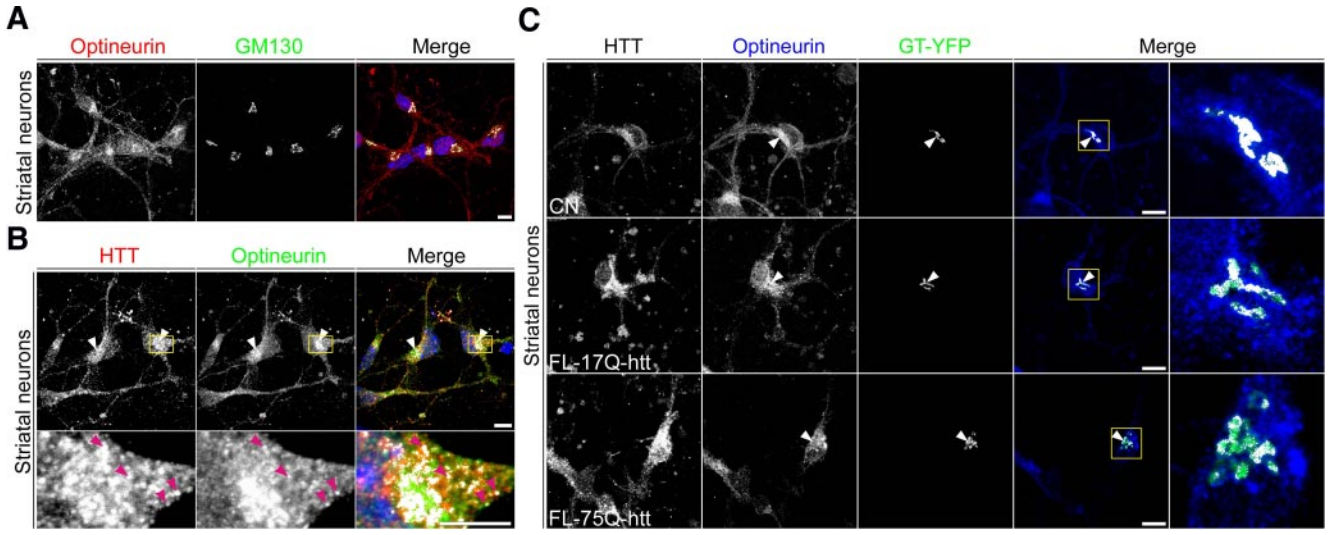

Figure 3. Full length mhtt reduces localization of optineurin in the Golgi apparatus of striatal neurons. (A) Double immunocytochemistry for optineurin and GM130 showed localization of optineurin in the Golgi complex of striatal neurons. (B) Optineurin colocalized with htt at the Golgi complex (arrowheads). Pink arrowheads indicate vesicles containing both proteins (enlarged region). (C) Colocalization of optineurin with GT-YFP showed reduced localization of optineurin in the Golgi apparatus in striatal neurons transfected with FL-75Q-htt and GT-YFP compared with those transfected with FL-17Q-htt and GT-YFP or GT-YFP alone (CN). Images represent the projection of the two slices containing the maximal cross-section of the cell nucleus. Bar, 8 μm.

apparatus, in knockin wt and mhtt cells. As shown in Figure 1, htt localized to the Golgi apparatus in wt cells and also in cytosolic vesicular structures. In contrast, mhtt cells displayed a 65% reduction in the colocalization between GT-YFP and htt compared with wt cells (Figure 1A). To confirm the delocalization of mhtt from the Golgi apparatus, wt cells were cotransfected with full-length htt (FL-17Q-htt) or mhtt (FL-75Q-htt) and GT-YFP. Localization of htt in the Golgi apparatus was observed in cells transfected with FL-17Q-htt. However, cells transfected with FL-75Q-htt showed a diffuse distribution of mhtt, with lower levels at the Golgi apparatus (Figure 1B). This observation was confirmed by Western blot of isolated Golgi membranes, which showed a decrease in htt protein levels in mhtt cells (Figure 1C; wt, 100 $\pm$ 26.6%; mhtt, 19.8 $\pm$ 4.4%, with respect to wt; $p < 0.01$). Given that both cell lines express similar levels of htt (Trettel *et al*., 2000), these findings are not attributable to a decrease in the total levels of htt in mhtt cells.

mhtt Reduces the Presence of Optineurin and Rab8 in the Golgi Apparatus

Optineurin, an htt-interacting protein, colocalizes with htt in the Golgi apparatus (Sahlender *et al*., 2005). Double immunocytochemistry for optineurin and the Golgi matrix protein GM130 showed that optineurin is mainly localized at the Golgi apparatus in wt cells (Figure 2A). Interestingly, we observed a delocalization of optineurin from the Golgi apparatus in mhtt cells, showing a 21% reduction compared with wt cells (Figure 2A). Consistent with this result, Western blot analysis showed no differences in the levels of total optineurin protein between wt and mhtt cells (Figure 2B; wt, 100 $\pm$ 14%; mhtt, 105 $\pm$ 9.4%, with respect to wt), whereas the protein levels of optineurin in isolated Golgi membranes were significantly reduced in mhtt cells (Figure 2B; wt, 100 $\pm$ 23%; mhtt, 41 $\pm$ 17%, with respect to wt; $p < 0.01$). In addition, double immunocytochemistry for htt and optineurin in wt cells showed colocalization of both proteins at the Golgi apparatus (Figure 2C, arrowheads) and also in vesicular structures (enlarged area shown in Figure 2C). In contrast, mhtt cells showed a punctate distribution of htt and optineurin and lower presence of both proteins at the Golgi apparatus (Figure 2C). In addition, mhtt cells showed a 32% decrease in the colocalization between these two proteins (Figure 2C, enlarged area).

We also examined the colocalization of optineurin and htt at the Golgi apparatus in other cell types. Double immunocytochemistry for optineurin and GM130 showed that optineurin is localized in the Golgi apparatus of striatal neurons (Figure 3A) and striatal rat-derived cell line (M213; Giordano *et al*., 1993) (Supplemental Figure 2A). Moreover, optineurin and htt colocalized at the Golgi apparatus (Figure 3B and Supplemental Figure 2B, arrowheads). In addition, both proteins were found in vesicles-like structures throughout the cytoplasm and also close to the Golgi apparatus (enlarged area shown in Figure 3B and Supplemental Figure 2B) in both cells.

To confirm the delocalization of optineurin from the Golgi apparatus caused by mhtt, cells were cotransfected with FL-17Q-htt or FL-75Q-htt and GT-YFP, or transfected with GT-YFP alone as a control condition. Reduced colocalization of optineurin with GT-YFP was observed in striatal neurons, wt cells, and M213 cells expressing FL-75Q-htt in comparison with those transfected with FL-17Q-htt or GT-YFP alone (Figures 3C, 4A, and Supplemental Figure 2C). Moreover, transfection of mhtt cells with FL-17Q-htt restored the normal levels of colocalization between optineurin and GT-YFP (Figure 4B), suggesting that htt is crucial for the localization of optineurin at the Golgi apparatus. To further corroborate this hypothesis, we next investigated the effects of depleting htt by siRNA. Consistent with previous studies (Caviston *et al*., 2007), we observed that wt cells transfected with htt siRNA showed partial Golgi disruption. Interestingly, the colocalization between optineurin and GT-YFP was lower in wt cells with reduced expression of htt with respect to those transfected with control siRNA (Figure 4C), indicating that htt is implicated in the localization of optineurin at the Golgi apparatus.

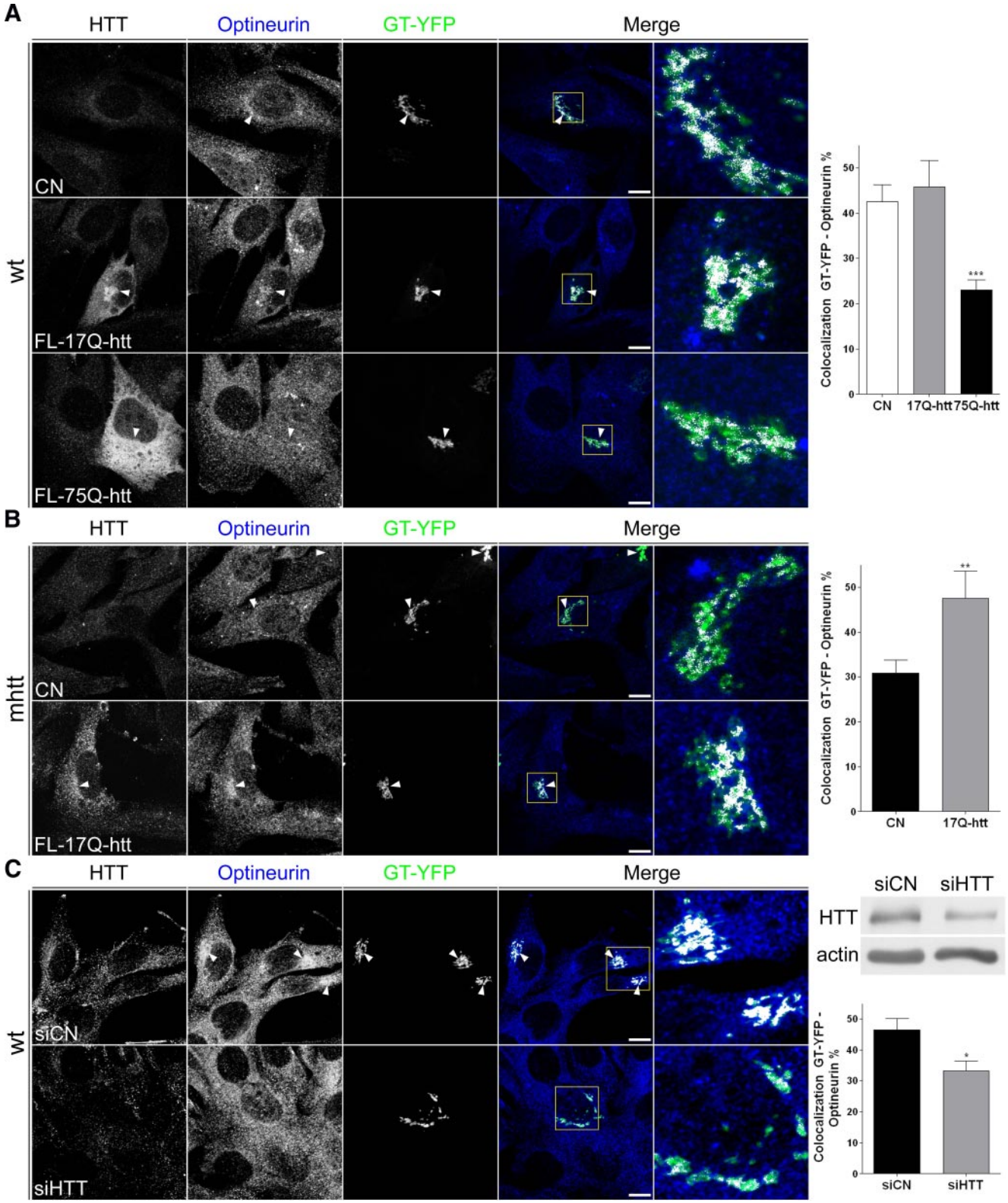

Figure 4. Full-length mhtt reduces localization of optineurin in the Golgi apparatus. This effect is reversed by full-length wild-type htt. (A) Colocalization of optineurin with GT-YFP showed reduced localization of optineurin in the Golgi apparatus in wt cells transfected with FL-75Q-htt and GT-YFP compared with cells transfected with FL-17Q-htt and GT-YFP or GT-YFP alone (CN). (B) mhtt cells transfected with FL-17Q-htt increased localization of optineurin in the Golgi apparatus compared with mhtt cells transfected with GT-YFP (CN). (C) Depletion of htt by siRNA reduced the colocalization of optineurin and GT-YFP. Representative Western blot showing reduced htt protein levels in cells transfected with htt siRNA is shown on the right side. Results are represented as a mean ± SEM determined from the analysis of three independent experiments (*$p < 0.05$; **$p < 0.01$; ***$p < 0.001$). Images represent the projection of the two slices containing the maximal cross section of the cell nucleus. Bar, 8 μm.

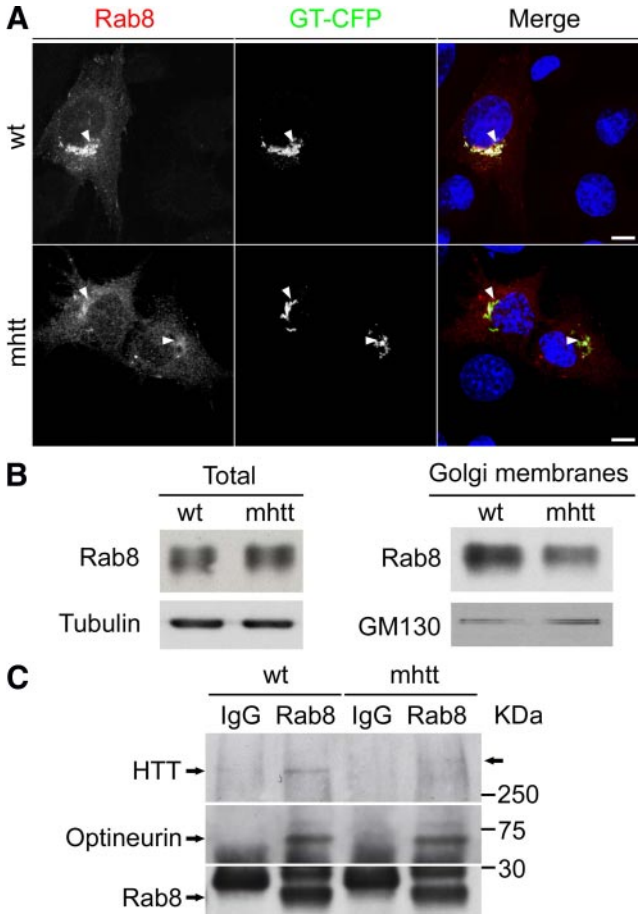

Figure 5. mhtt cells showed reduced localization of Rab8 in the Golgi apparatus. (A). wt and mhtt cells cotransfected with Rab8-GFP and GT-CFP. Rab8 is mainly located in the Golgi of wt cells. In contrast, mhtt cells showed lower levels of Rab8 in the Golgi apparatus. (B) Representative blot showing similar Rab8 protein levels in total extracts of wt and mhtt cells (20 μg each line) but reduced Rab8 protein levels in isolated Golgi membranes from the latter (10 μg each line). (C) Total extracts from wt and mhtt cells were immunoprecipipated using an anti-Rab8 antibody, revealing similar interaction between optineurin and Rab8 in both cells. Interaction between htt and the optineurin/Rab8 is reduced in mhtt cells as shown by decreased immunoprecipitation of htt in these cells. Images represent the projection of the two slices containing the maximal cross section of the cell nucleus. Bar, 8 μm.

In addition to htt, optineurin also interacts with Rab8 (Hattula and Peranen, 2000), which has been localized to the *trans*-Golgi network (TGN) (Huber *et al*., 1993), participating in post-Golgi trafficking (Ang *et al*., 2003). Thus, we next examined whether mhtt also alters the presence of Rab8 in the Golgi apparatus. Because Rab8 tagged with GFP has been used to determine Rab8 intracellular distribution (Ang *et al*., 2003; Sahlender *et al*., 2005), we determined the localization of Rab8 fused with GFP in wt and mhtt cells. Rab8 showed good colocalization around the Golgi apparatus in wt cells (Figure 5A). In contrast, mhtt cells showed lower levels of Rab8 in the Golgi apparatus (Figure 5A). These results were confirmed by Western blot analysis of isolated Golgi membranes. Total levels of Rab8 did not differ between wt and mhtt cells (Figure 5B; wt: 100 $\pm$ 8.3%; mhtt: 103 $\pm$ 16.8% with respect to wt), but protein levels of Rab8 in isolated Golgi membranes were reduced in the latter (Figure 5B; wt, 100 $\pm$ 3.7%; mhtt, 82 $\pm$ 1.3%, with respect to wt; $p < 0.05$).

The finding that optineurin and Rab8 were delocalized from the Golgi apparatus in the presence of mhtt, led us to assess whether the interaction between htt and the optineurin/Rab8 complex is altered in the presence of mhtt. Thus, we performed immunoprecipitation of Rab8 from wt and mhtt cell lysates (Figure 5C). In wt cells, we observed that both optineurin and htt were associated with Rab8, indicating that these proteins form a complex. Interestingly, the interaction between htt and the optineurin/Rab8 complex was lower in mhtt cells, although the presence of mhtt did not affect the interaction between optineurin and Rab8 (Figure 5C). These findings indicated reduced formation of the htt/optineurin/Rab8 complex in mhtt cells.

To further analyze the role of mhtt in the htt/optineurin/Rab8 complex, we next transfected wt and mhtt cell lines with a constitutively active Rab8-GTP-bound mutant form (Rab8 Q67L) and GT-CFP or GT-CFP alone as a control condition. This mutation alters Rab8-dependent trafficking (Peranen *et al*., 1996; Ang *et al*., 2003) by disrupting the localization of proteins involved in this transport such as AP-1B in polarized epithelial cells (Ang *et al*., 2003) and AP-1 in knockin striatal cells (wt cells; Supplemental Figure 3). Thus, we next examined whether expression of Rab8 Q67L alters the localization of htt and optineurin in both wt and mhtt cells. The wt cells cotransfected with Rab8 Q67L-GFP and GT-CFP showed a 37.5 and 27.8% reduction in the colocalization of optineurin and htt with GT-CFP, respectively (Figure 6). Interestingly, overexpression of Rab8 Q67L in mhtt cells did not result in additive impairment with the htt mutation (Figure 6). The lack of synergic effects suggested that the mutations of htt and Rab8 act in a similar manner on the Golgi apparatus. In agreement with that, expression of Rab8 Q67L (Peranen *et al*., 1996) or mhtt (Supplemental Figure 4A and Supplemental Movie 1) results in 28–30% reduction in the transport of VSV-G, a glycoprotein from the vesicular stomatitis virus, which is released from the Golgi apparatus to the plasma membrane.

Together, all these results suggest that mhtt alters the post-Golgi trafficking described previously (del Toro *al*., 2006), by uncoupling the htt/optineurin/Rab8 complex at the Golgi apparatus. To test this hypothesis, we next characterized whether mhtt affects the CCVs in the Golgi apparatus.

mhtt Alters Clathrin-dependent Post-Golgi Trafficking to Lysosomes

Optineurin and Rab8 participate in the regulated post-Golgi transport mediated by the AP-1 (Sahlender *et al*., 2005; Au *et al*., 2007). Thus, we examined whether mhtt affects AP-1 localization at the Golgi apparatus. Double immunocytochemistry for γ-adaptin, a specific subunit of AP-1, and mannosidase 2 (ManII), which marks the Golgi apparatus, showed an 18% higher colocalization in mhtt than in wt cells (Figure 7A). Consistent with this result, Western blot analysis showed no differences in the levels of total γ-adaptin protein between wt and mhtt cells, whereas the protein levels of γ-adaptin in isolated Golgi membranes were significantly increased in mhtt cells (Figure 7B). These findings suggest that clathrin-dependent post-Golgi trafficking is impaired, because AP-1 provides the first step of cargo-sequestration specificity in this route (Brodsky *et al*., 2001; McNiven and Thompson, 2006). Thus, we next examined the ultrastructure of the Golgi apparatus in wt and mhtt cells. The former showed the characteristic Golgi morphology of stacked flattened cisternae (Figure 7C). In contrast, in mhtt

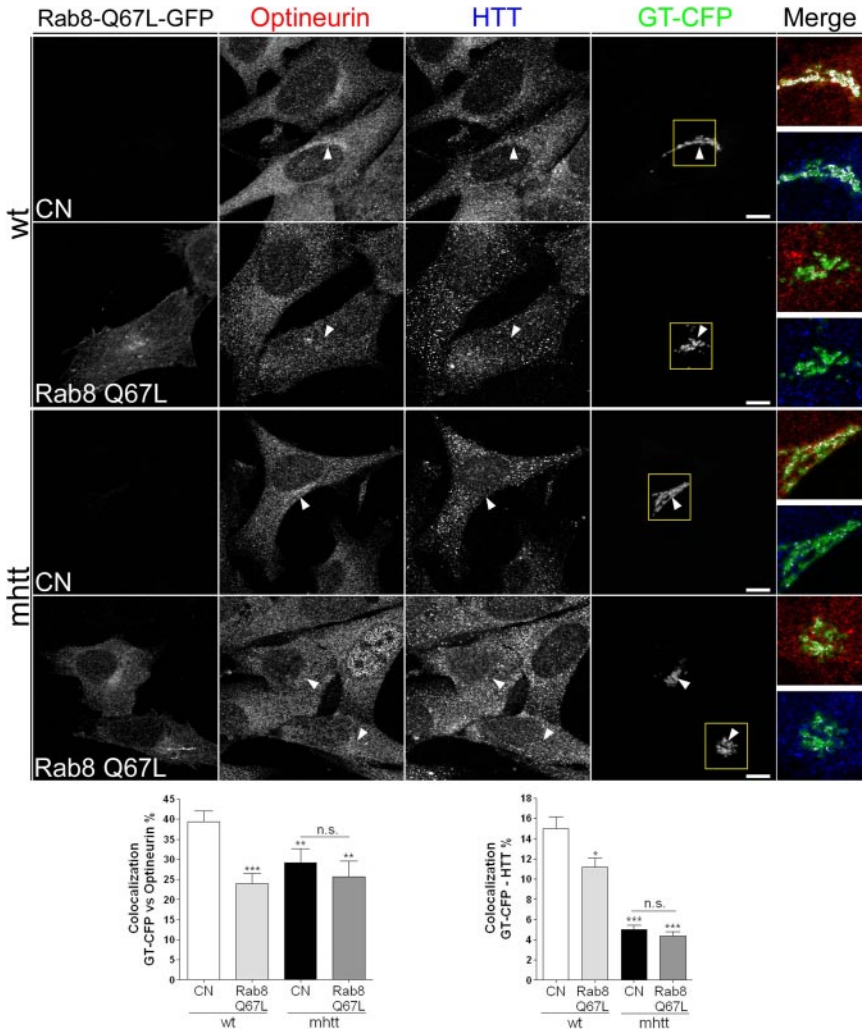

Figure 6. Rab8 Q67L reduces the localization of optineurin and htt in the Golgi apparatus in wt but not in mhtt cells. wt cells transfected with Rab8 Q67L showed reduced colocalization of optineurin or htt with GT-CFP. Conversely, no differences in the colocalization of either optineurin and mhtt with GT-CFP were observed between mhtt cells transfected or not with Rab8 Q67L, although both showed lower colocalization compared with wt cells. Results are represented as a mean ± SEM determined from the analysis of three independent experiments (n.s.; *$p < 0.05$; **$p < 0.01$; ***$p < 0.001$ vs. wt cells). Images represent the projection of the two slices containing the maximal cross-section of the cell nucleus. Bar, 8 μm.

cells the Golgi was partially disorganized showing high degree of vesiculation, although some cisternae remained stacked and flattened (Figure 7C). Interestingly, mhtt cells showed an abnormal accumulation of CCV profiles in proximity to Golgi cisternae (Figure 7C; wt, 0.19 ± 0.14 vs. mhtt, 0.87 ± 0.27 CCVs/μm^2; $p < 0.001$). We did not observe clathrin-coated budding profiles in mhtt cells, suggesting that there is not a deficit in CCV budding or fission. Notice that in wt cells, Golgi-associated CCV profiles were almost undetectable (Figure 7C). This result indicates a potential alteration in either CCV-mediated cargo transport or clathrin uncoating in mhtt cells and therefore points out to defects in AP-1–dependent post-Golgi trafficking.

To verify this hypothesis, we examined the intracellular distribution of Lamp-1, which uses the AP-1 complex-dependent pathway to lysosomes (Honing *et al*., 1996). mhtt cells showed increased colocalization between Lamp-1 and GT-YFP (Figure 7D). Given that both cell lines express similar levels of Lamp-1 as we observed by Western blot (data not shown), this result indicated an altered post-Golgi transport of Lamp-1. Consistently, iFRAP analysis showed a 37.4% reduction in the exit of Lamp-1 from the TGN in mhtt cells (Figure 7E, Table 1, and Supplemental Movie 2). To confirm the dependence of post-Golgi trafficking to lysosomes on the optineurin/Rab8 complex, we cotransfected Lamp-1 with Rab8 or the Rab8 Q67L mutant form in wt and mhtt cells and carried out iFRAP analysis. Overexpression of Rab8 did not induce significant differences in the post-Golgi transport of Lamp-1 with respect to cells not transfected with Rab8 (Figure 7F and Table 1). In contrast, wt cells expressing Rab8 Q67L showed a 44% reduction in the TGN egress of Lamp-1 compared with wt cells (Figure 7F and Table 1), which is consistent with the delocalization of htt and optineurin from de Golgi apparatus in the presence of Rab8 Q67L (Figure 6). Interestingly, no significant differences were found between mhtt cells, and either mhtt or wt cells expressing Rab8 Q67L (Figure 7F, Table 1, and Supplemental Movie 2). Together, these results suggest that mhtt impairs Rab8-dependent post-Golgi trafficking by means of a defect in the transport of CCVs from the TGN. In agreement with this view, iFRAP studies showed a 20% reduction in the exit of the LcB from the Golgi apparatus in mhtt (Table 1, Supplemental Figure 4B, and Supplemental Movie 3). This observation suggests that the disruption of the htt/optineurin/Rab8 complex by mhtt affects the assembly of CCVs with their motor proteins.

The impairment of TGN egress of cargos destined to lysosomes should affect the function of this compartment. Thus, we next examined whether the steady-state subcellular distribution of the MPR, which is determinant in transport of luminal lysosomal enzymes (Dahms *et al*., 1989), is altered by mhtt. Wt cells showed a widespread

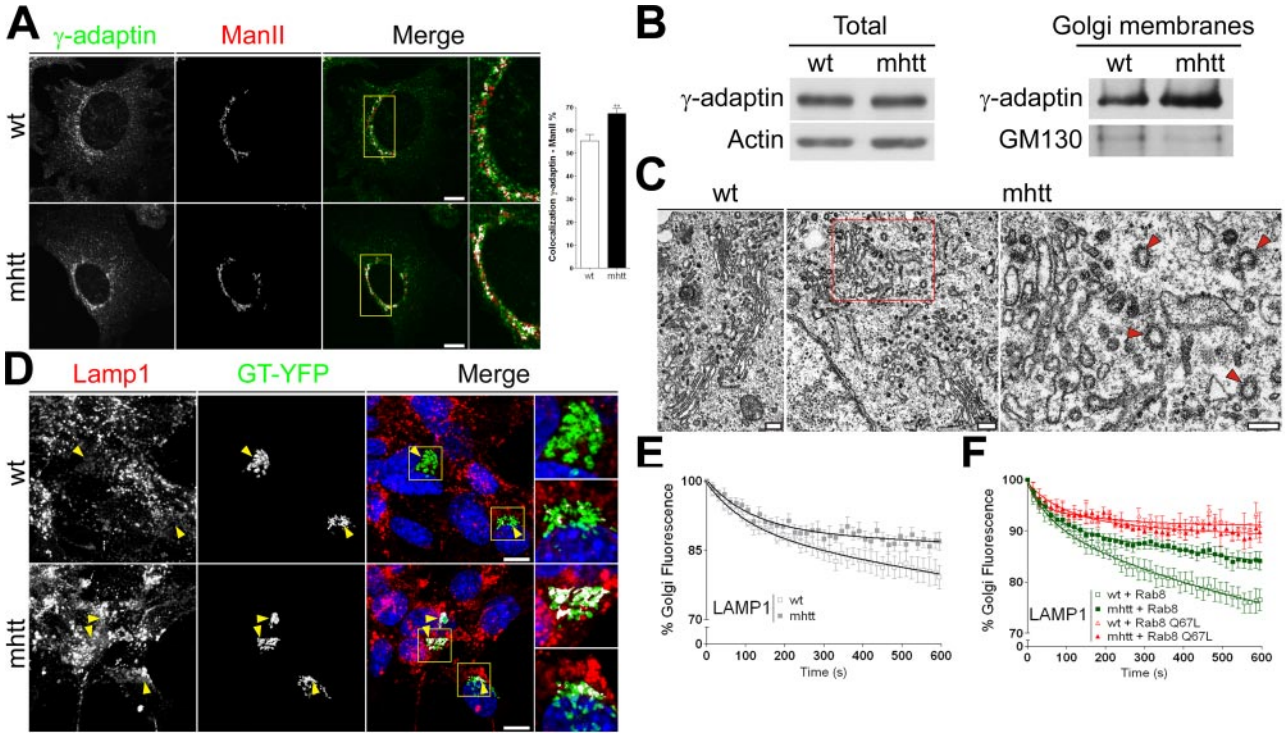

Figure 7. mhtt cells showed accumulation of AP-1 in the TGN, thereby impairing post-Golgi trafficking to lysosomes. (A) Colocalization between γ-adaptin, a specific subunit of AP-1, and ManII revealed increased accumulation of AP-1 in mhtt cells. (B) Representative blot showing similar γ-adaptin protein levels in total extracts of wt and mhtt cells (20 μg each line) but increased γ-adaptin protein levels in isolated Golgi membranes from the latter (10 μg each line). (C) Electron microscopy studies revealed a higher number of CCV profiles close to Golgi stacks of mhtt cells than in wt cells. Red arrows indicate CCVs profiles. (D) Increased colocalization between Lamp-1 and GT-YFP in mhtt cells. (E) Lamp-1 post-Golgi transport was reduced in mhtt cells compared with wt cells. (F) Expression of Rab8 do not alter the transport dynamics of Lamp-1 in either wt or mhtt cells. In contrast, overexpression of Rab8 Q67L impaired post-Golgi transport in wt cells. Moreover, mhtt cells transfected or not with Rab8 Q67L showed similar retention of Lamp-1 in the Golgi apparatus. Results are represented as a mean ± SEM determined from analysis of three independent experiments (**$p < 0.01$). Images represent the projection of the two slices containing the maximal cross section of the cell nucleus. Bar A, D: 8 μm; C: 200 nm.

distribution of MPR in the Golgi apparatus and in cytoplasmatic vesicular structures. In contrast, as shown in Figure 8A, mhtt cells retained the MPR labeling in the Golgi apparatus, displaying a 68% decrease in the number of MPR-containing cytosolic structures and a 260% increase in the colocalization between MPR and GM130 (Figure 8B). This altered subcellular distribution is indicative that post-Golgi transport of MPR is impaired in mhtt cells. In accordance to this result, iFRAP analyses for MPR showed a 30% decrease of TGN exit in mhtt cells (Figure 8C, Table 1, and Supplemental Movie 4). In addition, expression of FL-17Q-htt restored the post-Golgi transport of MPR in mhtt cells (Figure 8D, Table 1, and Supplemental Movie 5). To confirm the involvement of htt in the post-Golgi transport of MPR, we performed iFRAP analysis in wt cells with depletion of htt by siRNA. Wt cells with reduced expression of htt showed a 35% decrease of MPR post-Golgi transport (Figure 8E, Table 1, and Supplemental Movie 6). Consistent with these results, expression of FL-75Q-htt reduced the number MPR-containing cytosolic structures in wt cells in comparison to those transfected with FL-17Q-htt or GT-CFP alone (Figure 8F). Moreover, mhtt cells expressing FL-17Q-htt restored normal levels of MPR-containing cytosolic structures (Figure 8G). Together, these results indicate that, in mhtt cells, the loss of htt function impairs the post-Golgi transport of MPR.

Altered Lysosomal Function in mhtt Cells

To test the hypothesis that reduced post-Golgi transport of MPR could contribute to a deficit in the transport of enzymes to lysosomes, we next analyzed the number and the size of lysosomes using the LysoTracker, a marker for acidic compartments. A 22.3% reduction was observed in the number of LysoTracker-positive structures per mhtt cell compared with wt cells. However, we notice that the average size of the LysoTracker-positive structures in these mutant cells increased 17.8% over that of wt cells (Figure 9, A and B). We also examined the protein levels and maturation of cathepsin D, the predominant lysosomal aspartic acid protease (Saftig *et al*., 1995). Double immunocytochemistry for cathepsin D and LysoTracker showed a 63% decrease in the colocalization of these two markers in mhtt compared with wt cells (Figure 9, A and C). Cathepsin D is synthesized as procathepsin D (52 kDa), which is transported from the Golgi apparatus to lysosomes, in which it is processed to an active enzymatic form (48 kDa; Chinni *et al*., 1998). Thus, we examined by Western blot the total protein levels as well as the percentage of mature and immature cathepsin D forms versus total cathepsin D. mhtt cells showed a 43% decrease in the total protein levels of cathepsin D. Besides this decrease, the ratio of procathepsin D to total levels of cathepsin D increased 57% in mhtt compared with wt cells. In contrast, the ratio of mature cathepsin D to total levels decreased 14% in mhtt cells (Figure 9D). These results are indicative of

Table 1. Kinetic values and mobility fractions calculated for iFRAP experiments

Experimental condition		Golgi → late endosome/lysosome			
		Mobile fraction	K_1 constant	K_2 constant	$t_{1/2}$ (s)
Lamp1	wt	20.82 ± 2.52	5.1e−4	9.6e−3	172.6
	mhtt	13.03 ± 1.93*	1.5e−4	8.4e−3	103.7
Lamp1 Rab8	wt	23.5 ± 2.2	1.3e−3	1.7e−2	199.3
	mhtt	15.84 ± 1.89	4.2e−4	1.6e−2	108.1
Lamp1 Rab8 Q67L	wt	8.91 ± 2.87#	5.7e−3	4.4e−2	50.06
	mhtt	10.23 ± 2.3#	1.7e−4	9.9e−3	95.36
MPR	wt	46.81 ± 2.44	2.2e−3	3.3e−2	243.2
	mhtt	32.78 ± 3.92**	3.8e−4	7.7e−3	157.8
MPR CN	mhtt	34.94 ± 2.78	4.7e−4	1e−2	209.1
MPR FL-17Q -htt	mhtt	46.40 ± 2.94*	1e−3	8.2e−3	212.3
	wt	50.15 ± 3.58**	8.5e−4	8.4e−3	234.6
MPR	wt+siCN	49.52 ± 4.5	5.3e−4	6e−3	217.1
	wt+siHTT	31.92 ± 2.5**	1e−3	2.1e−2	379.9
LcB	wt	56.24 ± 1.72	4.2e−4	9.1e−3	125.6
	mhtt	45.47 ± 2.98*	6.8e−4	1.1e−2	99.23
VSV-G	wt	60.17 ± 4	1e−3	1.5e−2	341
	mhtt	43.38 ± 4.5*	6.3e−4	1e−2	198.2

iFRAP studies showing a reduced mobile fraction of Lamp-1 in mhtt cells compared to wt cells (see Figure 7E) (*$p < 0.05$ vs. wt cells). Coexpression of Rab8 Q67L reduced the mobile fraction of Lamp-1 in wt cells, whereas mhtt cells were not significantly affected (see Figure 7F) (#$p < 0.05$ vs. wt cells). MPR, LcB, and VSV-G expressed in mhtt cells showed a reduced mobile fraction compared with wt cells (see Figure 8C and Supplemental Figure 4, respectively) (**$p < 0.01$ vs. MPR in wt cells; *$p < 0.05$ vs. LcB in wt cells; *$p < 0.05$ vs. VSV-G in wt cells). Expression of FL-17Q-htt restored mobile fraction of MPR in mhtt cells (Figure 8D) (*$p < 0.05$, **$p < 0.01$ vs. MPR in mhtt cells). Reduced levels of htt by siRNA reduced the mobile fraction of MPR in wt cells (Figure 8E) (**$p < 0.01$ vs. MPR in wt cells expressing control siRNA).

altered transport of procathepsin D from the TGN to lysosomes in mhtt cells, which is supported by immunocytochemistry and iFRAP results of Lamp-1 and MPR (Figures 7 and 8).

We next tested whether lysosomal function could be altered in mhtt cells. Thus, we incubated mhtt and wt cell lines with the quenched fluorescent substrate DQ-collagen IV, which is degraded in lysosomes and gives rise to intense fluorescence (Sameni *et al*., 2000). mhtt cells showed fewer fluorescent punctae cytoplasmatic structures than wt cells. This observation indicated a reduced proteolysis of DQ-collagen IV, which implies altered lysosome functionality (Figure 9E).

Altered lysosome activity has been shown to induce autophagic stress (Zhang *et al*., 2007). Thus, we investigated whether the enlarged LysoTracker-positive structures found in mhtt cells could be in fact autophagic vacuoles. Therefore, we incubated wt and mhtt cells with MDC, which is a marker for autophagic vacuoles (Biederbick *et al*., 1995) as well as LysoTracker to stain acidic compartments. mhtt cells showed increased staining of MDC-positive structures, which were colocalized with enlarged LysoTracker-positive structures (Figure 10A), suggesting an increase in autophagic vacuoles. To confirm these results we performed electron microscopy studies. We observed that mhtt cells presented autophagic vacuoles possessing part of the cytoplasm or granular deposits. We also found fingerprint profiles (Figure 10B) and structures surrounded by double-layered membranes (Figure 10, C–E). Together, these results indicate that mhtt cells have altered lysosome activity and increased autophagic vacuole-like structures.

DISCUSSION

We have previously shown that htt plays a crucial role in the regulation of post-Golgi trafficking (del Toro *et al*., 2006). However, the mechanism by which mhtt impairs this regulated exocytic process is not known. Here, we show that mhtt impairs the optineurin/Rab8-dependent secretory pathway, which in turn alters clathrin-mediated post-Golgi exit. Thus, mhtt influences not only the regulated secretion to the plasma membranes (del Toro *et al*., 2006) but also the lysosomal route, which in turn leads to lysosomal dysfunction.

Our experiments showed that htt is located in the Golgi apparatus and also in transport vesicles, which is in agreement with previous studies (Difiglia *et al*., 1995; Gauthier *et al*., 2004). In addition, our results show that mhtt has a reduced localization in the Golgi apparatus with respect to htt. This observation is consistent with reduced interaction between mhtt and HIP14, a palmitoyl transferase that facilitates htt interaction with Golgi membranes (Huang and El-Husseini, 2005; Yanai *et al*., 2006). Interestingly, we observed that delocalization of mhtt was accompanied with reduced levels of optineurin in the Golgi apparatus. Consistently, expression of full-length htt restored the levels of

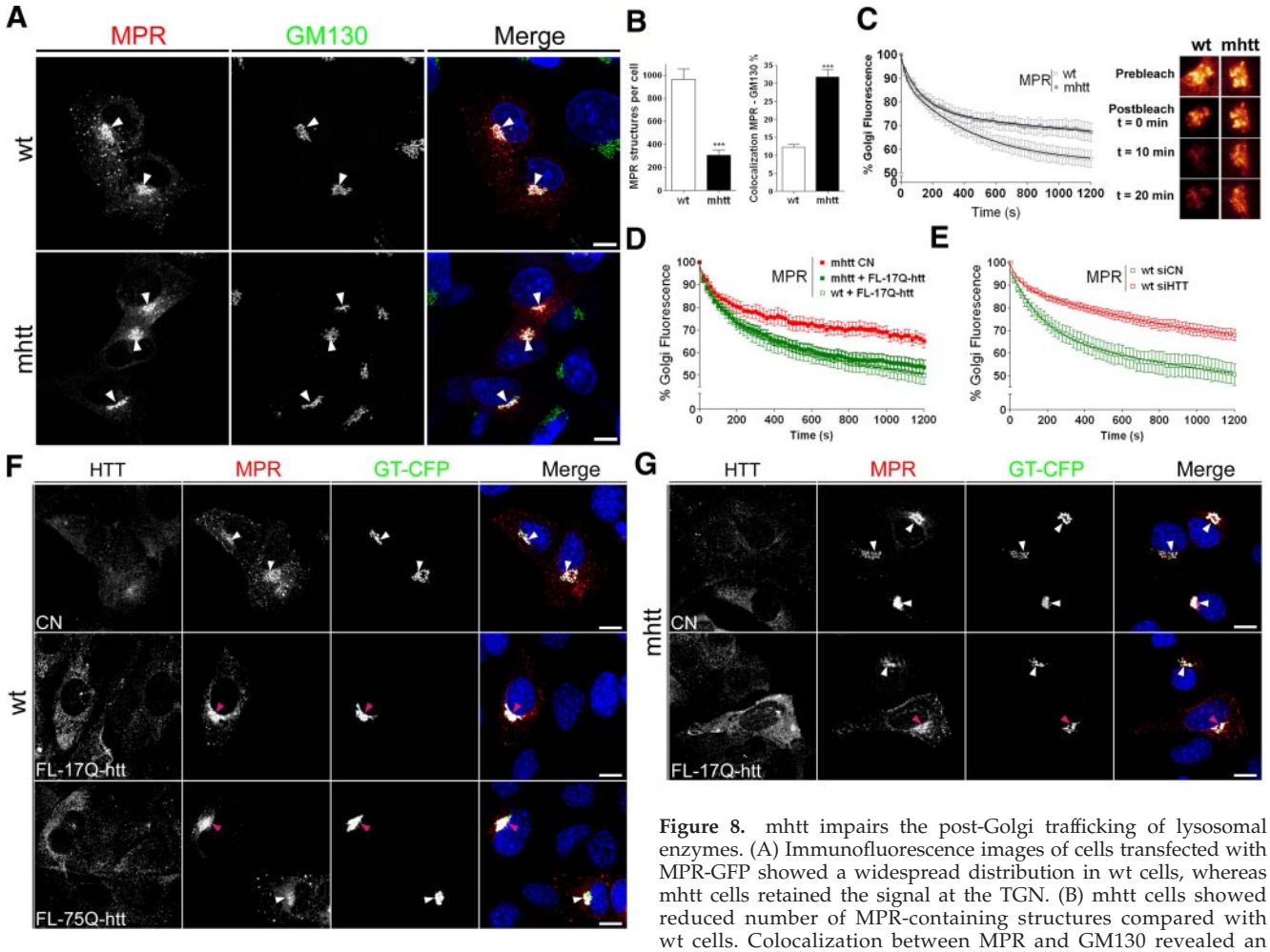

Figure 8. mhtt impairs the post-Golgi trafficking of lysosomal enzymes. (A) Immunofluorescence images of cells transfected with MPR-GFP showed a widespread distribution in wt cells, whereas mhtt cells retained the signal at the TGN. (B) mhtt cells showed reduced number of MPR-containing structures compared with wt cells. Colocalization between MPR and GM130 revealed an accumulation of MPR at the Golgi complex in mhtt cells. (C) MPR showed reduced post-Golgi transport in mhtt cells compared with wt cells. Representative Golgi apparatus fluorescence for each condition is shown on the right side. (D) Expression of FL-17Q-htt restored the post-Golgi transport of MPR in mhtt cells. (E) Depletion of htt by siRNA impair the post-Golgi transport of MPR in wt cells. (F) Reduced number of MPR-positive vesicles in wt cells transfected with FL-75Q-htt and GT-YFP compared with cells transfected with FL-17Q-htt and GT-YFP or GT-YFP alone (CN). (G) mhtt cells transfected with FL-17Q-htt showed widespread distribution of MPR compared with mhtt cells transfected with GT-YFP (CN). Pink arrows mark cells expressing FL-17Q-htt or FL-75Q-htt. Results are represented as a mean ± SEM determined from analysis of three independent experiments (***$p < 0.001$ for MPR in mhtt vs. wt cells). Images represent the projection of the two slices containing the maximal cross section of the cell nucleus. Bar, 8 μm.

optineurin in the Golgi of mhtt cells. The fact that htt interacts with optineurin (Hattula and Peranen, 2000) and also with the Golgi membranes, suggest that htt may play a central role in the correct localization and function of optineurin in the Golgi apparatus. This is in agreement with our observation that silencing htt by siRNA delocalized optineurin from the Golgi apparatus.

In addition to optineurin, mhtt also delocalized Rab8 from the Golgi apparatus. Rab8 belongs to the family of Rab GTPases and plays an important role in the post-Golgi transport (Ang *et al*., 2003). Because htt interacts directly with optineurin but not with Rab8 (Hattula and Peranen, 2000), one possible explanation for the delocalization of Rab8 from the Golgi apparatus in mhtt cells is the decrease of optineurin in this compartment. In keeping with this view, immunoprecipitation studies showed reduced interaction between mhtt and the optineurin/Rab8. However, the optineurin-Rab8 interaction was not affected by the presence of mhtt. Together, these results suggest that htt plays an important role in the localization of optineurin/Rab8 at the Golgi apparatus. Optineurin and Rab8 are essential for post-Golgi trafficking (Ang *et al*., 2003; Sahlender *et al*., 2005). In support, depletion of optineurin by RNAi or overexpression of Rab8Q67L result in altered post-Golgi trafficking of the VSV-G (Peranen *et al*., 1996; Sahlender *et al*., 2005). Similarly, mhtt affects the clathrin-dependent post-Golgi trafficking (del Toro *et al*., 2006), including the post-Golgi transport of VSV-G (present study). Therefore, the reduced interaction between mhtt and the optineurin/Rab8 complex together with the mislocalization of these proteins in mhtt cells, perturbs the functionality of the Golgi apparatus.

CCVs emanate from the TGN to deliver cargos to the cell surface or to lysosomes (for review, see Pfeffer, 2003). Electron microscopy images showed partial disruption of the Golgi apparatus that could be related to the reduction of optineurin and htt in this apparatus. In fact, depletion of optineurin or htt results in Golgi disorganization (Sahlender *et al*., 2005; Caviston *et al*., 2007). Interestingly, there is an abnormal increase in CCVs in the proximity of the TGN in mhtt cells. This finding suggests that CCVs do not leave the

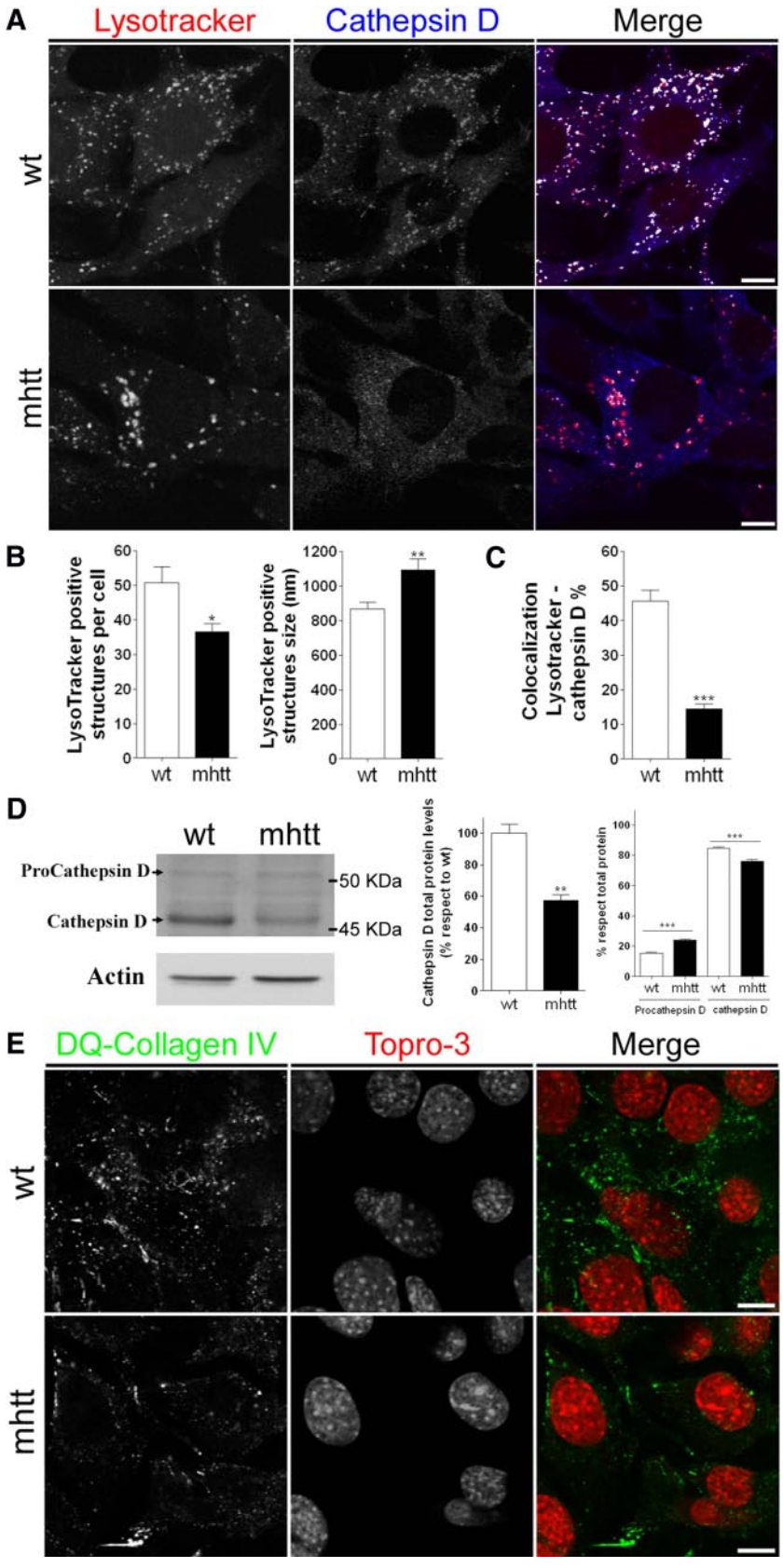

Figure 9. mhtt cells showed altered lysosome morphology and lower lysosomal content of cathepsin D. (A) wt and mhtt cells were immunostained using anti-cathepsin D antibody and LysoTracker. (B) Quantification of morphological studies revealed a reduced number of LysoTracker-positive structures of greater size in mhtt cells. (C) Colocalization studies showed decreased localization of cathepsin D in LysoTracker-positive structures of mhtt cells compared with wt cells. (D) Representative blot showing procathepsin D and cathepsin D protein levels in total extracts of wt and mhtt cells (30 μg each line). mhtt cells showed lower total levels of cathepsin D. In addition, mhtt cells showed higher levels of procathepsin D but lower levels of mature cathepsin D. (E) mhtt cells showed reduced lysosomal activity. wt and mhtt cells were incubated during 2 h in the presence of 25 μg/ml quenched DQ-Collagen-IV. mhtt cells showed a reduced number of green fluorescent dots, which are indicative of DQ-Collagen-IV degradation. Results are represented as a mean ± SEM determined from analysis of three independent experiments (*$p < 0.05$; **$p < 0.01$; ***$p < 0.001$ vs. wt cells). Images represent the projection of the two slices containing the maximal cross section of the cell nucleus. Bar, 8 μm.

TGN correctly. Supporting this notion is the accumulation of AP-1 a clathrin adaptor complex, in the Golgi apparatus of mhtt cells, which was accompanied by reduced egress of clathrin from the TGN as showed the iFRAP analysis. Thus,

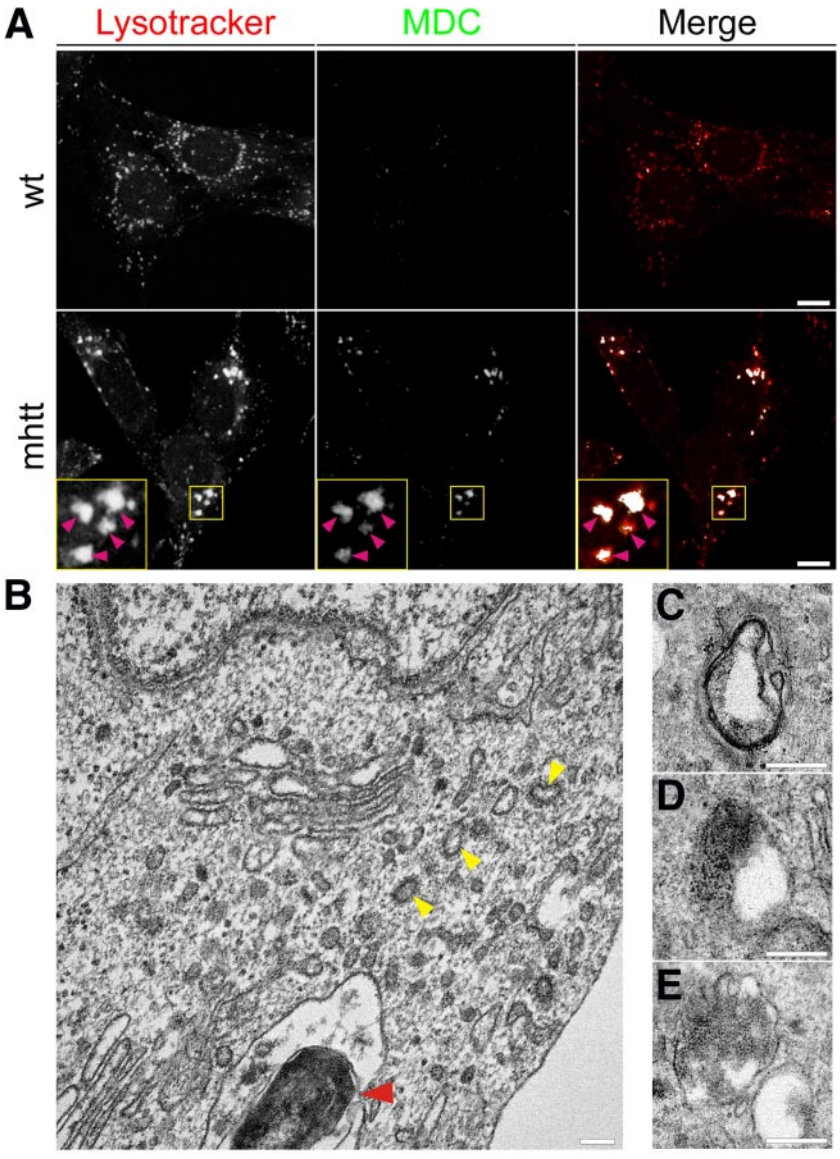

Figure 10. mhtt cells showed increased intracellular autophagosomes. (A) MDC staining, which marks autophagic vacuoles, colocalized with enlarged lysosomes marked with LysoTracker in mhtt cells. (B) Electron microscopy studies revealed the presence of autophagic vacuoles-like structures in mhtt cells. (B) Red arrow indicates a fingerprint profile. Also note the presence of CCVs profiles (yellow arrows). (C–E) Different autophagic vacuoles present in mhtt cells. Bar A: 8 μm; B–E: 200 nm.

it is plausible that alteration of the htt/optineurin/Rab8 complex by mhtt impairs the correct motion of CCVs from the TGN. This hypothesis is supported by the observation that optineurin interacts with myosin VI (Sahlender *et al*., 2005), which acts as an actin based motor for the transport of vesicles that exit from the TGN (Au *et al*., 2007). In addition, htt binds to dynein and HAP-1 facilitating the motility of vesicles along microtubules (Caviston *et al*., 2007). Thus, alteration of the htt/optineurin/Rab8 complex affects the correct motion of CCVs from the TGN because of a lack of interaction with their motors, which would explain the retention of secretory proteins in the TGN of mhtt cells (del Toro *et al*., 2006; Figure 11).

Thus, it is reasonable to hypothesize that the reduction in the transport of CCVs from the TGN alters the trafficking of lysosomal proteins. Our findings demonstrate that mhtt impairs the post-Golgi trafficking of Lamp-1 and MPR. Moreover, expression of Rab8Q67L affected the post-Golgi trafficking of Lamp-1 to a similar degree as mhtt. This finding is in agreement with the delocalization of htt and optineurin from the Golgi apparatus in the presence of Rab8 Q67L in wt cells, which suggests that constitutively active Rab8 interferes with the normal cycle of nucleotide binding and hydrolysis altering the functionality/location of its effectors (Ang *et al*., 2003). Interestingly, no additive effects were observed when Rab8 Q67L was expressed in mhtt cells. The lack of synergic effects indicates that the mhtt affects lysosomal transport via optineurin/Rab8 complex. MPR transports newly synthesized lysosomal hydrolases bearing mannose 6-phosphate from the TGN to late endosomes or prelysosomes (Dahms *et al*., 1989). Consistent with altered post-Golgi transport of MPR, mhtt cells showed an incorrect processing of procathepsin D, which in turn reduced the levels of mature cathepsin D in lysosomes. These findings are coincident with the reduction of lysosomal activity observed in mhtt cells. Interestingly, we observed that overexpression of truncated forms of mhtt, such as exon1–103Q-htt, stimulated post-Golgi transport of Lamp-1 and also increased the labeling of cathepsin D in enlarged LysoTracker-positive structures (Supplemental Figure 5), which is in agreement with a previous study (Kegel *et al*., 2000). This effect could be explained by several protein interactions that

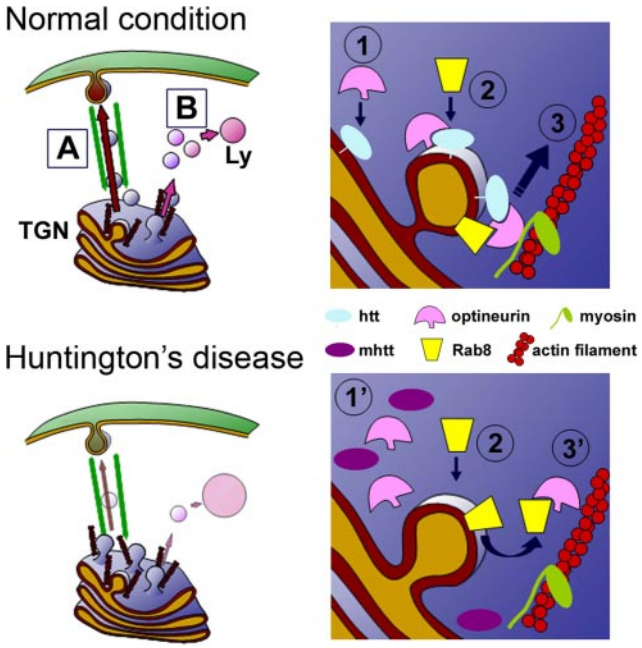

Figure 11. Proposed model of the effects of mhtt on post-Golgi trafficking to the plasma membrane (A) and to the lysosomes (B). In normal conditions, palmitoylated htt facilitates the location of optineurin in the Golgi apparatus (1). The interaction of Rab8 with the htt/optineurin complex stabilizes Rab8 in the Golgi apparatus (2). Htt/Optineurin/Rab8 complex allows the correct interaction of CCVs with motors, which in turn promotes the scission of the vesicle and its transport (3). In HD, mhtt is not correctly located in the Golgi apparatus, which causes a reduction in the presence of optineurin (1′). The lack of the htt–optineurin complex in the Golgi apparatus impairs the correct stabilization of the Rab8 in the Golgi apparatus (3′), producing an accumulation of CCVs in this compartment.

are lost in the case of shorter fragments of htt. In fact, shorter fragments of mhtt do not modify intracellular transport (Gauthier *et al*., 2004; Colin *et al*., 2008) or post-Golgi trafficking (del Toro *et al*., 2006).

It has been shown that macroautophagy, a large-scale catabolic mechanism, is required to clear mhtt aggregates (Rubinsztein *et al*., 2007). In fact, stimulation of autophagy by rapamycin is protective in HD models (Ravikumar *et al*., 2004) and has been proposed as a therapeutic strategy for this disease (Rubinsztein, 2006). Macroautophagy requires the fusion of autophagosomes with lysosomes to degrade the proteins into the autophagolysosome (Rubinsztein *et al*., 2007). Therefore, the results reported here could provide a link to explain the reduced lysosome activity with an impaired macroautophagy in HD. Consistently, mhtt cells showed an increase in autophagic vacuoles similar to those seen in cathepsin D-deficient mice, which exhibit dramatic autophagic stress (Koike *et al*., 2005).

In conclusion, our findings demonstrate that htt participates in the clathrin coated-mediated post-Golgi trafficking through the optineurin/Rab8 complex. mhtt delocalizes the optineurin/Rab8 complex from the Golgi apparatus, thereby impairing post-Golgi trafficking to the lysosomal pathway, which could contribute to defects in lysosome functionality in HD.

ACKNOWLEDGMENTS

We thank M. Teresa Muñoz and Ana López for technical assistance and Dr. Maria Calvo from the confocal microscopy unit at the Serveis Científico-Tècnics (Universitat de Barcelona) for support and advice on confocal techniques. We also express our appreciation to Dr. Juan S. Bonifacino for the mannose-6 phosphate receptor and clathrin light chain constructs, Dr. Jennifer Lippincott-Schwartz for the galactosyltransferase construct, Dr. Ira Mellmann for the Rab8 Q67L construct, Dr. Kai Simons for VSV-G, and Drs. Fréderic Saudou and Sandrine Humbert for full length wild-type and mutant htt constructs. We thank Dr. Marcy MacDonald for striatal-derived cells and Dr. William Freed for M213 cells. Robin Rycroft checked the English. This study was supported by grants from the Ministerio de Educación y Ciencia (SAF2005-01335, to J. A.; BFU2006-00867, to G. E.; SAF2006-04202, to J.M.C.; Spain), the Ministerio de Sanidad y Consumo [CIBERNED, to J. A.; and RETICS (Red de Terapia Celular), to J.M.C.; Spain], and the Fundació La Marató de TV3 (to J. A.; Spain).

REFERENCES

Ang, A. L., Folsch, H., Koivisto, U. M., Pypaert, M., and Mellman, I. (2003). The Rab8 GTPase selectively regulates AP-1B-dependent basolateral transport in polarized Madin-Darby canine kidney cells. J. Cell Biol. *163*, 339–350.

Au, J. S., Puri, C., Ihrke, G., Kendrick-Jones, J., and Buss, F. (2007). Myosin VI is required for sorting of AP-1B-dependent cargo to the basolateral domain in polarized MDCK cells. J. Cell Biol. *177*, 103–114.

Balch, W. E., Dunphy, W. G., Braell, W. A., and Rothman, J. E. (1984). Reconstitution of the transport of protein between successive compartments of the Golgi measured by the coupled incorporation of N-acetylglucosamine. Cell *39*, 405–416.

Biederbick, A., Kern, H. F., and Elsasser, H. P. (1995). Monodansylcadaverine (MDC) is a specific in vivo marker for autophagic vacuoles. Eur. J. Cell Biol. *66*, 3–14.

Brodsky, F. M., Chen, C. Y., Knuehl, C., Towler, M. C., and Wakeham, D. E. (2001). Biological basket weaving: formation and function of clathrin-coated vesicles. Annu. Rev. Cell Dev. Biol. *17*, 517–568.

Canals, J. M., Pineda, J. R., Torres-Peraza, J. F., Bosch, M., Martin-Ibanez, R., Munoz, M. T., Mengod, G., Ernfors, P., and Alberch, J. (2004). Brain-derived neurotrophic factor regulates the onset and severity of motor dysfunction associated with enkephalinergic neuronal degeneration in Huntington's disease. J. Neurosci. *24*, 7727–7739.

Caviston, J. P., Ross, J. L., Antony, S. M., Tokito, M., and Holzbaur, E. L. (2007). Huntingtin facilitates dynein/dynactin-mediated vesicle transport. Proc. Natl. Acad. Sci. USA *104*, 10045–10050.

Chinni, S. R., Gercel-Taylor, C., Conner, G. E., and Taylor, D. D. (1998). Cathepsin D antigenic epitopes identified by the humoral responses of ovarian cancer patients. Cancer Immunol. Immunother. *46*, 48–54.

Colin, E., Zala, D., Liot, G., Rangone, H., Borrell-Pages, M., Li, X. J., Saudou, F., and Humbert, S. (2008). Huntingtin phosphorylation acts as a molecular switch for anterograde/retrograde transport in neurons. EMBO J. *27*, 2124–2134.

Dahms, N. M., Lobel, P., and Kornfeld, S. (1989). Mannose 6-phosphate receptors and lysosomal enzyme targeting. J. Biol. Chem. *264*, 12115–12118.

del Toro, D., Canals, J. M., Gines, S., Kojima, M., Egea, G., and Alberch, J. (2006). Mutant huntingtin impairs the post-Golgi trafficking of brain-derived neurotrophic factor but not its Val66Met polymorphism. J. Neurosci. *26*, 12748–12757.

Difiglia, M., *et al*. (1995). Huntingtin is a cytoplasmic protein associated with vesicles in human and rat brain neurons. Neuron *14*, 1075–1081.

Dundr, M., Hoffmann-Rohrer, U., Hu, Q., Grummt, I., Rothblum, L. I., Phair, R. D., and Misteli, T. (2002). A kinetic framework for a mammalian RNA polymerase in vivo. Science *298*, 1623–1626.

Fernandez-Ulibarri, I., Vilella, M., Lazaro-Dieguez, F., Sarri, E., Martinez, S. E., Jimenez, N., Claro, E., Merida, I., Burger, K. N., and Egea, G. (2007). Diacylglycerol is required for the formation of COPI vesicles in the Golgi-to-ER transport pathway. Mol. Biol. Cell. *18*, 3250–3263.

Gauthier, L. R., *et al*. (2004). Huntingtin controls neurotrophic support and survival of neurons by enhancing BDNF vesicular transport along microtubules. Cell *118*, 127–138.

Giordano, M., Takashima, H., Herranz, A., Poltorak, M., Geller, H. M., Marone, M., and Freed, W. J. (1993). Immortalized GABAergic cell lines derived from rat striatum using a temperature-sensitive allele of the SV40 large T antigen. Exp. Neurol. *124*, 395–400.

Hattula, K., and Peranen, J. (2000). FIP-2, a coiled-coil protein, links Huntingtin to Rab8 and modulates cellular morphogenesis. Curr. Biol. *10*, 1603–1606.

Hoffner, G., Kahlem, P., and Djian, P. (2002). Perinuclear localization of huntingtin as a consequence of its binding to microtubules through an interaction with beta-tubulin: relevance to Huntington's disease. J. Cell Sci. *115*, 941–948.

Honing, S., Griffith, J., Geuze, H. J., and Hunziker, W. (1996). The tyrosine-based lysosomal targeting signal in lamp-1 mediates sorting into Golgi-derived clathrin-coated vesicles. EMBO J. *15*, 5230–5239.

Huang, K., and El-Husseini, A. (2005). Modulation of neuronal protein trafficking and function by palmitoylation. Curr. Opin. Neurobiol. *15*, 527–535.

Huber, L. A., Pimplikar, S., Parton, R. G., Virta, H., Zerial, M., and Simons, K. (1993). Rab8, a small GTPase involved in vesicular traffic between the TGN and the basolateral plasma membrane. J. Cell Biol. *123*, 35–45.

Kegel, K. B., Kim, M., Sapp, E., McIntyre, C., Castano, J. G., Aronin, N., and Difiglia, M. (2000). Huntingtin expression stimulates endosomal-lysosomal activity, endosome tubulation, and autophagy. J. Neurosci. *20*, 7268–7278.

Koike, M., *et al*. (2005). Participation of autophagy in storage of lysosomes in neurons from mouse models of neuronal ceroid-lipofuscinoses (Batten disease). Am. J. Pathol. *167*, 1713–1728.

Kremer, B., *et al*. (1994). A worldwide study of the Huntington's disease mutation. The sensitivity and specificity of measuring CAG repeats. N. Engl. J. Med. *330*, 1401–1406.

McNiven, M. A., and Thompson, H. M. (2006). Vesicle formation at the plasma membrane and trans-Golgi network: the same but different. Science *313*, 1591–1594.

Peranen, J., Auvinen, P., Virta, H., Wepf, R., and Simons, K. (1996). Rab8 promotes polarized membrane transport through reorganization of actin and microtubules in fibroblasts. J. Cell Biol. *135*, 153–167.

Pfeffer, S. (2003). Membrane domains in the secretory and endocytic pathways. Cell *112*, 507–517.

Ravikumar, B., *et al*. (2004). Inhibition of mTOR induces autophagy and reduces toxicity of polyglutamine expansions in fly and mouse models of Huntington disease. Nat. Genet. *36*, 585–595.

Rubinsztein, D. C. (2006). The roles of intracellular protein-degradation pathways in neurodegeneration. Nature *443*, 780–786.

Rubinsztein, D. C., Gestwicki, J. E., Murphy, L. O., and Klionsky, D. J. (2007). Potential therapeutic applications of autophagy. Nat. Rev. Drug Discov. *6*, 304–312.

Saftig, P., *et al*. (1995). Mice deficient for the lysosomal proteinase cathepsin D exhibit progressive atrophy of the intestinal mucosa and profound destruction of lymphoid cells. EMBO J. *14*, 3599–3608.

Sahlender, D. A., Roberts, R. C., Arden, S. D., Spudich, G., Taylor, M. J., Luzio, J. P., Kendrick-Jones, J., and Buss, F. (2005). Optineurin links myosin VI to the Golgi complex and is involved in Golgi organization and exocytosis. J. Cell Biol. *169*, 285–295.

Sameni, M., Moin, K., and Sloane, B. F. (2000). Imaging proteolysis by living human breast cancer cells. Neoplasia *2*, 496–504.

Sharp, A. H., *et al*. (1995). Widespread expression of Huntington's disease gene (IT15) protein product. Neuron *14*, 1065–1074.

Singaraja, R. R., *et al*. (2002). HIP14, a novel ankyrin domain-containing protein, links huntingtin to intracellular trafficking and endocytosis. Hum. Mol. Genet. *11*, 2815–2828.

Stenmark, H., and Olkkonen, V. M. (2001). The Rab GTPase family. Genome Biol. *2*, REVIEWS3007.

Trettel, F., Rigamonti, D., Hilditch-Maguire, P., Wheeler, V. C., Sharp, A. H., Persichetti, F., Cattaneo, E., and MacDonald, M. E. (2000). Dominant phenotypes produced by the HD mutation in STHdh(Q111) striatal cells. Hum. Mol. Genet. *9*, 2799–2809.

Yanai, A., *et al*. (2006). Palmitoylation of huntingtin by HIP14 is essential for its trafficking and function. Nat. Neurosci. *9*, 824–831.

Zhang, L., *et al*. (2007). Small molecule regulators of autophagy identified by an image-based high-throughput screen. Proc. Natl. Acad. Sci. USA *104*, 19023–19028.